

Landau velocity for collective quantum Hall breakdown in bilayer graphene: Supplemental Material

W. Yang,¹ H. Graef,^{1,2} X. Lu,³ G. Zhang,³ T. Taniguchi,⁴ K. Watanabe,⁴
A. Bachtold,⁵ E.H.T. Teo,⁶ E. Baudin,¹ E. Bocquillon,¹ G. Fève,¹
J-M. Berroir,¹ D. Carpentier,⁷ M. O. Goerbig,⁸ and B. Plaçais^{1,*}

¹*Laboratoire Pierre Aigrain, Ecole normale supérieure,
PSL University, Sorbonne Université,
Université Paris Diderot, Sorbonne Paris Cité,
CNRS, 24 rue Lhomond, 75005 Paris France*

²*CINTRA, UMI 3288, CNRS/NTU/Thales,
Research Techno Plaza, 50 Nanyang Drive, Singapore 637553*

³*Beijing National Laboratory for Condensed Matter Physics and Institute of Physics,
Chinese Academy of Sciences, Beijing 100190, China*

⁴*Advanced Materials Laboratory, National Institute for
Materials Science, Tsukuba, Ibaraki 305-0047, Japan*

⁵*ICFO - Institut de Ciències Fotoniques,
The Barcelona Institute of Science and Technology,
08860 Castelldefels, Barcelona, Spain*

⁶*Nanyang Technol Univ, Sch Elect and Elect Engn,
50 Nanyang Ave, Singapore 639798, Singapore*

⁷*Univ. Lyon, ENS de Lyon, Univ. Claude Bernard,
CNRS, Laboratoire de Physique, F-69342, France*

⁸*Laboratoire de Physique des Solides,
CNRS UMR 8502, Univ. Paris-Sud,
Université Paris-Saclay, F-91405 Orsay Cedex, France*

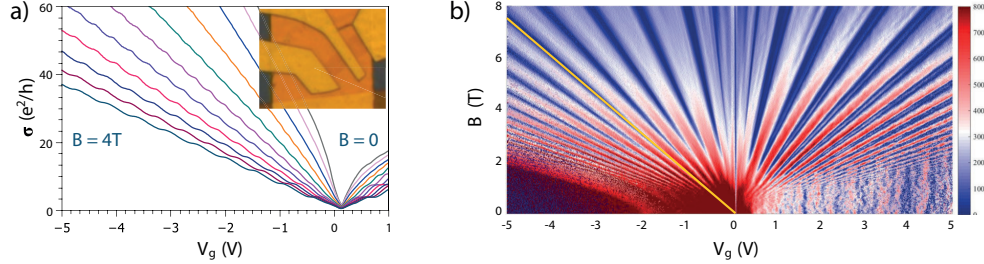


FIG. 1: Low-field magnetotransport in bilayer graphene at $T = 4$ K. a) Conductance quantization steps (at $V_{ds} = 3$ mV in units of $4e^2/h$) of the 2-terminal bottom gated bilayer graphene on 23 nm-thick boron nitride (BN) device of dimensions $L \times W = 4 \times 3 \mu\text{m}$ (optical image in the inset). The tiny width of the quantum Hall plateaus warrants the absence of disorder-induced localized bulk states. b) Fan chart of the zero-field differential conductance $\partial G_{ds}/\partial V_g$ ($\mu\text{S}/\text{V}$) showing a series of Landau levels ($N = -10 \rightarrow 10$, the yellow line signals the median $N = 5$ state) and the lifting of their 4-fold degeneracy of the $N = 0$ state.

I. SAMPLE FABRICATION

Our sample is fabricated from BLG chosen here as a prototypical massive ($m^*/m_0 \simeq 0.03$) 2D electron system with a Landau ladder of inter-LL gap $\hbar\omega_c \lesssim 30$ meV for $B \lesssim 8$ T. Boron nitride (BN) dielectric provides a high mobility $\mu = 3 \text{ m}^2\text{V}^{-1}\text{s}^{-1}$ ($T = 4$ K), a smooth electrostatic environment, and an enhanced thermal stability against the high currents and E -fields used in this work [1]. These points are central as they favor homogeneous breakdown over the surface, and high-quality breakdown measurements. A local bottom gate allows tuning the number of occupied LLs in a broad range $N \lesssim 10$, while efficiently screening the substrate charge disorder. These statements are supported by several observations. First the electrostatic smoothness is evidenced by the small size of the zero-bias quantization plateaus in Supp. Fig.1-a and their smearing at low bias $V_{ds} \gtrsim 5$ mV. Secondly, the fan chart $\partial G_{ds}(V_{gs}, B)/\partial V_g$ in Supp. Fig.1-b, is characteristic of clean BLG with a low quantizing threshold $B \gtrsim 2$ T and a lifting of the fourfold degeneracy of the $N = 0$ state. A typical working condition is the ($B = 4$ T ; $V_g = -3$ V) point in the middle of the experimental window corresponding to $N \simeq 5$ and $n \simeq -2 \cdot 10^{12} \text{ cm}^{-2}$ in Supp. Fig.1-b. The breakdown is monitored by measuring the transport current and the shot noise as described in Ref.[1]. It is expressed as a noise current $S_I/2e$ in the Fig.1 of the main text for an easy comparison with transport currents presented in the same panel.

The 2-terminal sample, of dimensions $L \times W = 4 \times 3 \mu\text{m}$, is an as-exfoliated BLG flake stacked on a 23 nm-thick BN crystal deposited on a metallic bottom gate (see optical picture in Supp. Fig.1-a inset). The sample is equipped with low-resistance ($R_c \simeq 120 \Omega \cdot \mu\text{m}$) Pd/Au contacts (see Fig.1 in Ref.[1]), and embedded in a coplanar wave guide for 0–10 GHz cryogenic (4 K) noise measurement. Shot noise is measured in the 4.5–5.5 GHz band (see Supplementary of Ref.[1]). The high-frequency band is needed to overcome the colored low frequency noise that obscures shot noise up to ~ 1 GHz at the maximum bias current. Carrier density is compensated for drain gating as explained in Ref.[1]. The dissipation-less Hall regime is characterized by a 2-terminal conductance G_{ds} matching the Hall conductance $G_H = |n|e/B$. QHE plateaus are used to calibrate the gate capacitance $C_g \simeq 1.15 \text{ mF}/\text{m}^2$.

The $B = 0$ transport and noise properties have been characterized in a previous report (Ref.[1]) where a new cooling mechanism could be revealed and experimental techniques were detailed.

II. MAGNETO-EXCITONS IN CROSSED MAGNETIC AND ELECTRIC FIELDS

Magneto-excitons are collective electron-hole excitations that arise in 2D electronic systems in a strong magnetic field. They are the zeros of the dielectric function,

$$\epsilon_E(\mathbf{q}, \omega) = 0 \simeq 1 - \frac{e^2}{\epsilon q} \Pi_E^0(\mathbf{q}, \omega), \quad (1)$$

where the last expression is that obtained within the random-phase approximation (RPA), in terms of the polarizability $\Pi_E^0(\mathbf{q}, \omega)$ for non-interacting electrons. Here, the subscript indicates that we consider a non-zero electric field that we choose to be oriented in the y -direction.

A. Polarizability

We have

$$\Pi_E^0(\mathbf{q}, \omega) = \frac{1}{\hbar S} \sum_{\nu, \nu'} \frac{P_\nu - P_{\nu'}}{\omega - (\varepsilon_\nu - \varepsilon_{\nu'}) + i\eta} |\psi_\nu^\dagger e^{i\mathbf{q}\cdot\mathbf{r}} \psi_{\nu'}|^2, \quad (2)$$

where S denotes de total surface, P_ν is the Fermi-Dirac occupation number of the level ε_ν and ψ_ν the associated eigenstate. The latter are labelled by the quantum numbers $\nu = (\lambda, n, k)$, which in our case include the band index λ , the Landau level index n , and the wave vector $k = k_x$. Here, we consider the Landau gauge $\mathbf{A} = B(-y, 0, 0)$ for the vector potential because of our choice to apply an electric field in the y -direction. Finally, η denotes a small level broadening. Equation (2) is generic for the usual 2D electron gas, monolayer or bilayer graphene. The latter case is of interest here, and we have $\varepsilon_\nu = \lambda \hbar \omega_c \sqrt{n(n-1)} + \hbar v_D k$, where $v_D = E/B$ is the drift velocity, and the wave functions

$$\psi_\nu = \frac{1}{\sqrt{2}} \begin{pmatrix} |n-2, k\rangle \\ \lambda |n, k\rangle \end{pmatrix} \quad (3)$$

where the states $|n, k\rangle$ are simply the solutions of the Hamiltonian²

$$H = \frac{p_y^2}{2m^*} + \frac{1}{2} m^* \omega_c^2 (y - y_0)^2 + \hbar v_D k, \quad (4)$$

in terms of the average position $y_0 = kl_B^2 - v_D/\omega_c$ and the magnetic length $l_B = \sqrt{\hbar/eB}$.

In the present experiment, the bilayer graphene system is substantially doped, and the last occupied Landau level $N \gg 1$. In this limit we can approximate the matrix elements

$$\psi_{\lambda, n, k}^\dagger e^{i\mathbf{q}\cdot\mathbf{r}} \psi_{\lambda, n', k'} \simeq \langle n, k | e^{i\mathbf{q}\cdot\mathbf{r}} | n', k' \rangle, \quad (5)$$

the corrections being on the order of $1/N$, and neglect interband contributions to the polarizability (2). The matrix elements can be calculated with the help of the wave functions

$$\langle x, y | n, k \rangle = \frac{1}{\sqrt{L}} e^{ikx} \chi_n(y - y_0), \quad (6)$$

where $\chi_n(y) = H_n(y/l_B) \exp(-y^2/2l_B^2)$ in terms of the Hermite polynomial H_n , and one obtains

$$\langle n, k | e^{i\mathbf{q}\cdot\mathbf{r}} | n', k' \rangle = \delta_{k, k'+q_x} \int dy e^{iq_y y} \chi_n(y - kl_B^2 + v_D/\omega_c) \chi_{n'}(y - k'l_B^2 + v_D/\omega_c). \quad (7)$$

The delta term indicates momentum conservation in the x -direction, and one notices that the electric field only enters here in the form of an irrelevant shift that disappears by a variable transformation $y' = y - v_D/\omega_c$ in the integral. This means that the electric field does not alter the matrix elements with respect to the $E = 0$ case, apart from a phase factor $\exp(-i\varphi)$, with $\varphi = q_y v_D/\omega_c$, and it only tilts the energy levels as a function of k [see Eq. (4)]. We emphasize that this property also holds if we had not used the approximation (5). The matrix elements can now be obtained in the standard manner [2] and read, for $n' \geq n$,⁸

$$\langle n, k | e^{i\mathbf{q}\cdot\mathbf{r}} | n', k' \rangle = \delta_{k, k'+q_x} e^{-i\varphi} e^{\frac{i}{2}q_y(k+k')l_B^2} e^{-|\alpha|^2/2} \sqrt{\frac{n'}{n}} (-\alpha^*)^{n-n'} L_{n'}^{n-n'}(|\alpha|^2), \quad (8)$$

in terms of the associated Laguerre polynomials L_n^m and the complex wave vector $\alpha = (q_x + iq_y)l_B/\sqrt{2}$. Notice that all phase factors disappear once we take the modulus square in the expression for the polarizability, which becomes

$$\Pi_E^0(\mathbf{q}, \omega) = \frac{1}{\hbar S} \sum_{n, n'; k} \frac{P_{n, k} - P_{n', k-q_x}}{\omega - [(n - n')\omega_c + v_D q_x] + i\eta} |\langle n, k | e^{i\mathbf{q}\cdot\mathbf{r}} | n', k - q_x \rangle|^2. \quad (9)$$

The last expression is still difficult to evaluate because of the Fermi-Dirac occupation numbers. However, just below the breakdown threshold, the system is not at thermodynamic equilibrium, and we consider the Fermi level to be quenched between two adjacent Landau levels even if they are tilted with respect to k (see Supp. Fig. 2),

$$P_{n, k} = P_n = \Theta(N - n), \quad (10)$$

in terms of the step function $\Theta(N - n) = 1$ for $n \leq N$ and $\Theta(N - n) = 0$ for $n > N$. This allows us now to carry out the sum over the quantum number k , and with $\sum_k = N_B = n_B S$, in terms of the flux density $n_B = eB/h = 1/2\pi l_B^2$, we obtain the final expression

$$\Pi_E^0(\mathbf{q}, \omega) = \frac{n_B}{\hbar} \sum_{n, n'} \frac{P_n - P_{n'}}{(\omega - v_D q_x) - (n - n')\omega_c + i\eta} \mathcal{F}_{n, n'}(q) \quad (11)$$

for the polarizability, where we have defined the form factor

$$\begin{aligned} \mathcal{F}_{n, n'}(q) = & \Theta(n - n') \frac{n!}{n'} \left(\frac{q^2 l_B^2}{2} \right)^{n-n'} \left[L_{n'}^{n-n'} \left(\frac{q^2 l_B^2}{2} \right) e^{-q^2 l_B^2/4} \right]^2 \\ & + \Theta(n' - n) \frac{n!}{n'} \left(\frac{q^2 l_B^2}{2} \right)^{n'-n} \left[L_n^{n'-n} \left(\frac{q^2 l_B^2}{2} \right) e^{-q^2 l_B^2/4} \right]^2. \end{aligned} \quad (12)$$

B. Collective excitations

Let us discuss in more detail the obtained result for the polarizability (11) in the presence of an electric field. The expression is insofar extremely useful in that we find the same result

as in the absence of an electric field, $E = 0$, but at a different frequency $\omega \rightarrow \omega - v_D q_x$. The electric field thus has the sole effect to shift the energies by $-\hbar v_D q_x$, and we find quite generally

$$\Pi_E^0(\mathbf{q}, \omega) = \Pi_{E=0}^0(\mathbf{q}, \omega - \mathbf{v}_D \cdot \mathbf{q}) \quad (13)$$

and consequently

$$\epsilon_E(\mathbf{q}, \omega) = \epsilon_{E=0}(\mathbf{q}, \omega - \mathbf{v}_D \cdot \mathbf{q}), \quad (14)$$

as mentioned in the main text. The collective excitations therefore satisfy, before the breakdown transition, Galilean invariance, and their dispersion reads

$$\omega_{ME}^E(\mathbf{q}) = \omega_{ME}^{E=0}(\mathbf{q}) - \mathbf{v}_D \cdot \mathbf{q}, \quad (15)$$

where $\omega_{ME}^{E=0}(\mathbf{q})$ is the dispersion in the absence of an electric field.

While this analysis is valid for any type of collective electron-hole excitation, we now concentrate on magneto-excitons, i.e. excitations that are adiabatically connected to the poles $m\omega_c$ at zero wave vector. In order to obtain these excitations, with $m = (n - n')$, we can restrict the sum in Eq. (11) to the relevant terms – we simply need to analyze the $E = 0$ case in view of the above discussion,

$$\Pi_{E=0}^0(\mathbf{q}, \omega) = \frac{n_B}{\hbar} \sum_{m=1}^{\infty} \sum_{n=0}^{m-1} \frac{2m\omega_c}{\omega^2 - m^2\omega_c^2} \mathcal{F}_{N-n}^m(q). \quad (16)$$

Under the above-mentioned assumption of adiabatic connection to the pole $m\omega_c$, we can omit the sum over m in the calculation of the zeros of the dielectric function, and one obtains

$$\omega_m^{E=0}(q)^2 - m^2\omega_c^2 \simeq 2m\omega_c \frac{e^2 n_B}{\hbar \epsilon q} \sum_{n=0}^{m-1} \mathcal{F}_{N-n}^m(q). \quad (17)$$

Linearization of this equation, which is strictly speaking valid in the limit $r_s = 1/a_B^* k_F = e^2/\epsilon l_B \sqrt{2N} \hbar \omega_c \ll 1^3$, yields the magneto-exciton⁴ dispersion

$$\omega_m^{E=0}(q) \simeq m\omega_c + \frac{1}{2\pi\hbar} \frac{e^2}{\epsilon q l_B^2} \sum_{n=0}^{m-1} \mathcal{F}_{N-n}^m(q), \quad (18)$$

and for the fundamental magneto-exciton ($m = 1$), we obtain

$$\begin{aligned} \omega_{ME}^{E=0}(q) &\simeq \omega_c + \frac{1}{2\pi\hbar} \frac{e^2}{\epsilon q l_B^2} \frac{q^2 l_B^2}{2(N+1)} \left[L_N^1 \left(\frac{q^2 l_B^2}{2} \right) e^{-q^2 l_B^2/4} \right]^2 \\ &\simeq \omega_c \left\{ 1 + \frac{r_s}{2\pi} \frac{\sqrt{2N}}{q l_B} \left[J_1(q l_B \sqrt{2N}) \right]^2 \right\} \\ &\simeq \omega_c \left\{ 1 + \frac{r_s}{2\pi} \frac{k_F}{q} \left[J_1(2Nq/k_F) \right]^2 \right\}, \end{aligned} \quad (19)$$

where we have used the asymptotic large- N behavior of the Laguerre polynomial

$$\frac{1}{N} L_N^1(x) \simeq \frac{1}{\sqrt{Nx}} J_1(2\sqrt{Nx}),$$

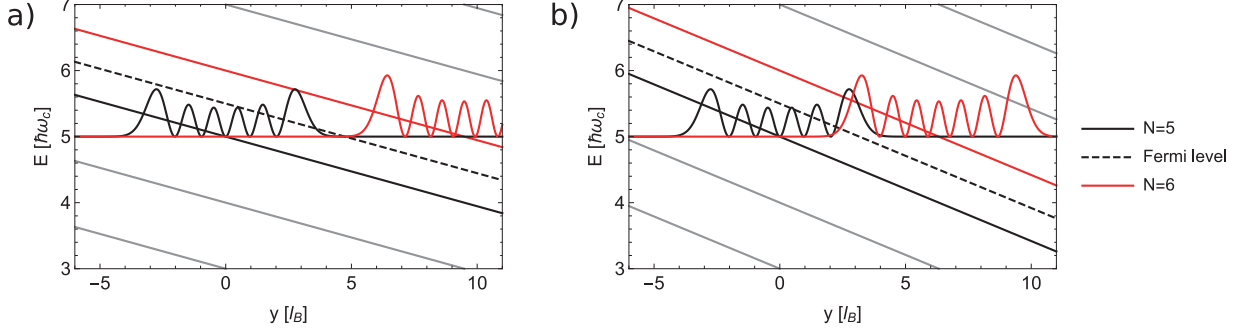


FIG. 2: Sketch of the Landau levels and their associated wave functions below (a) and at (b) the breakdown transition. Due to the electric field, the Landau levels are tilted but the Fermi level (dashed line) is quenched between N and $N + 1$, due to lack of possible equilibration. (a) Below breakdown, the magneto-exciton remains gapped at wave vectors that correspond to average distances between the electron and the hole constituting the magneto-exciton that are larger than the sum of the typical wave-function extensions. (b) Once the wave functions substantially overlap, i.e. at a magneto-exciton wave vector $ql_B \sim 2\sqrt{2N}$, upon increase of the electric field, the system becomes unstable to proliferation of magneto-excitons.

where J_1 is a Bessel function, and we have expressed the dispersion in terms of the Fermi wave vector $k_F = \sqrt{2N}/l_B$ in the last line.

The magneto-exciton dispersion in the presence of an in-plane electric field is then readily obtained from Eq. (15),

$$\begin{aligned} \omega_{ME}^E(q) &\simeq \omega_c \left\{ 1 + \frac{r_s}{2\pi} \frac{\sqrt{2N}}{ql_B} \left[J_1(ql_B\sqrt{2N}) \right]^2 \right\} - \mathbf{v}_D \cdot \mathbf{q} \\ &\simeq \omega_c \left\{ 1 + \frac{r_s}{2\pi} \frac{k_F}{q} \left[J_1(2Nq/k_F) \right]^2 \right\} - \mathbf{v}_D \cdot \mathbf{q}. \end{aligned} \quad (20)$$

This dispersion is depicted in Fig. 3(b) of the main text for several values of the electric field.

We finally notice that our calculation of the magneto-exciton dispersion does not provide information about their spectral weight and thus their visibility and pertinence in the $\omega - q$ plane. Here, we can nevertheless rely on calculations performed in the RPA for the full polarizability $\Pi(\mathbf{q}, \omega) = \Pi^0(\mathbf{q}, \omega)/\epsilon(\mathbf{q}, \omega)$, at $E = 0$ ^{3,5} that show that the spectral weight $\text{Im}\Pi(\mathbf{q}, \omega)$ is essentially restricted to an area of allowed particle-hole excitations⁶ delimited by $\omega_L \simeq v_F q$ and $\omega_R \simeq v_F(q - 2k_F)$, where $v_F = \hbar k_F/m^*$ is the Fermi velocity and where we have neglected a parabolic contribution that becomes relevant only at large values of $\omega \sim N\omega_c$. For the magneto-exciton of frequency $\omega_{ME} \sim \omega_c$, the spectral weight is therefore concentrated in interval $q_{min} \leq q \leq q_{max}$, with $q_{min} \simeq \omega_c/v_F \simeq 1/l_B\sqrt{2N}$ and $q_{max} \simeq 2k_F + \omega_c/v_F \simeq 2\sqrt{2N}/l_B$.

This behavior of the spectral weight can also be understood from a wave-function point of view (see Fig. 2). Indeed, the average distance ΔR between the centers of the ringlike wave functions of the electron (in level $N + 1$) and that of the hole (in level N) is related to the wave vector of the particle-hole pair $\Delta R = ql_B^2$ ⁶. Furthermore, the radii of the ringlike wave functions are $\sqrt{2(N + 1) + 1}l_B$ and $\sqrt{2N + 1}l_B$ for the electron and the hole, respectively. Therefore, the electron and the hole have a substantial overlap as long as the

average distance is between the radii difference and sum, $\sqrt{2(N+1)+1}l_B - \sqrt{2N+1}l_B \leq \Delta R \leq \sqrt{2(N+1)+1}l_B + \sqrt{2N+1}l_B$, which yields in the large- N limit the same criterion

$$1/\sqrt{2N} \leq ql_B \leq 2\sqrt{2N} \quad (21)$$

for the wave-vector range of strong spectral weight. The system therefore becomes unstable towards proliferation of magneto-excitons, that thus trigger the breakdown phenomenon, when the dispersion becomes negative at the wave vector q_{max} , i.e. $\omega_{ME}^E(q_{max}) \leq 0$ or

$$v_D q_{max} \simeq \omega_c \quad \Leftrightarrow \quad v_D = E/B \simeq \omega_c l_B / 2\sqrt{2N}. \quad (22)$$

III. FANO FACTOR

In contrast with the Zener mechanism, the proliferation of inter-LL collective excitations is naturally explained by the ME instability. However a quantitative determination of the number $N_{bunch} = \mathcal{F} \lesssim 20$ of excitation bunches remains beyond the scope of the present argument. This would require a comprehensive theory of the polarizability at high E -field and of the contribution to electric transport of the collective excitations. Moreover, experimental feedback would require a knowledge of the bias-dependent Hall angle which is not accessible in 2-terminal RF measurements. Still we can propose a tentative explanation which estimates the electrostatic back-action from the inter-edge charging energy $\varepsilon_c \sim e^2/(\epsilon W) \simeq 2$ meV, assuming an instantaneous bulk to edge counter drift of electron/hole partners after an elementary ME bunch creation. In this simple picture, the local E -field is transiently reduced below the breakdown threshold, stopping the excitation bunch, whenever the Coulomb potential $N_{bunch}\varepsilon_c$ compensates for a Landau gap unit, i.e. $N_{bunch} = \mathcal{F} \sim \hbar\omega_c/\varepsilon_c$ in order of magnitude accordance with experiment. Such a relaxation-oscillation mechanism bears analogies with the Frank-Condon mechanism in nanoelectronics where giant Fano factors are considered under phonon-triggered tunneling events [7].

* Electronic address: bernard.placais@lpa.ens.fr

¹ W. Yang, S. Berthou, X. Lu, Q. Wilmart, A. Denis, M. Rosticher, T. Taniguchi, K. Watanabe, G. Fève, J.-M. Berroir, G. Zhang, C. Voisin, E. Baudin and B. Plaçais, *Nature Nanotech.* **13**, 47-52 (2018). *A graphene Zener-Klein transistor cooled by a hyperbolic substrate*

² M. O. Goerbig, *Quantum Hall Effects*, in C. Miniatura et al. (ed.), *Ultracold Gases and Quantum Information*, Les Houches 2009, Oxford UP (Oxford); arXiv:0909.1998.

³ M.O. Goerbig, *Rev. Mod. Phys.* **83**, 1193 (2011). *Electronic properties of graphene in a strong magnetic field*

⁴ C. Kallin and B.I. Halperin, *Phys. Rev. B* **30**, 5655 (1984). *Excitations from a filled Landau level in the two-dimensional electron gas*; *Phys. Rev. B* **31**, 3635 (1985). *Many-body effects on the cyclotron resonance in a two-dimensional electron gas*

⁵ G. F. Giuliani and G. Vignale, *Quantum Theory of the Electron Liquid*, Cambridge UP (Cambridge, UK).

⁶ R. Roldán, M. O. Goerbig, and J.-N. Fuchs, *Semicond. Sci. Technol.* **25**, 034005 (2010).

⁷ J. Koch and F. von Oppen, *Phys. Rev. Lett.* **94**, 206804 (2005). *Franck-Condon Blockade and Giant Fano Factors in Transport through Single Molecules*

⁸ For $n' > n$, one simply needs to take the complex conjugate and interchange n and n' .